

# Convolutional Recurrent Neural Network Based Progressive Learning for Monaural Speech Enhancement

Andong Li<sup>a,b</sup>, Chengshi Zheng<sup>a,b,\*</sup>, Xiaodong Li<sup>a,b</sup>

<sup>a</sup>*Key Laboratory of Noise and Vibration Research, Institute of Acoustics, Chinese Academy of Sciences, 100190, Beijing, China*

<sup>b</sup>*University of Chinese Academy of Sciences, 100049, Beijing, China*

---

## Abstract

Recently, progressive learning has shown its capacity of improving speech quality and speech intelligibility when it is combined with deep neural network (DNN) and long short-term memory (LSTM) based monaural speech enhancement algorithms, especially in low signal-to-noise ratio (SNR) conditions. Nevertheless, due to a large number of parameters and highly computational complexity, it is hard to implement in current resource-limited micro-controllers and thus, it is important to significantly reduce both the amount of parameters and the computational load for practical applications. For this purpose, we propose a novel progressive learning framework with convolutional recurrent neural networks called PL-CRNN, which takes advantages of both convolutional neural networks and recurrent neural networks to drastically reduce the amount of parameters and simultaneously improve speech quality and speech intelligibility. Numerous experiments verify the effectiveness of proposed PL-CRNN model and indicate that it yields consistent better performance than the PL-DNN and PL-LSTM algorithms and also it gets results close even better than the CRNN in terms of various evaluation metrics. Compared with PL-DNN, PL-LSTM and state-of-the-art CRNN models, the proposed PL-CRNN algorithm can reduce the amount of parameters up to 77%, 93% and 93%, respectively.

---

\*Corresponding author

Email address: [cszheng@mail.ioa.ac.cn](mailto:cszheng@mail.ioa.ac.cn) (Chengshi Zheng)

*Keywords:* speech enhancement, deep learning, progressive learning, convolutional neural network, long short-term memory

---

## 1. Introduction

Environmental noise and speech reverberation are two major factors that have significantly influences on robust automatic speech recognition (ASR), speech communication system and hearing implants [1]. To improve speech recognition accuracy and speech communication quality in real scenarios, speech enhancement algorithms are proposed to extract the desired speech from its noisy equivalent to improve signal-to-noise ratio (SNR). Conventional monaural speech enhancement methods include spectral subtraction [2], Wiener filtering [3], subspace-based methods [4] and so on. It is well-known that the performance of these methods usually suffers from heavily decreased performance in extremely low SNR and non-stationary noise conditions, and it has already shown that these conventional speech enhancement algorithms cannot improve speech intelligibility for normal-hearing (NH) listeners [5].

In recent years, deep neural network (DNN)-based speech enhancement algorithms have attracted wide attention and their improved versions have been investigated owing to its superior potentials in complicated nonlinear mapping problems. DNN-based monaural speech enhancement algorithms are often categorized into two types, where one is spectral mapping approach [6, 8] and the other is mask mapping approach [9]. Motivated by the processing of human auditory system [12], Wang et.al [11] regard time-frequency (T-F) mask as a mapping target of DNN and learn an optimal mask function with data-driven methods. Ideal binary mask (IBM) [13], which is a type of hard-decision mask that classifies the value in each T-F unit as either 0 or 1 depending on whether SNR in the local region exceeds a predefined threshold or not. IBM faces some problems, for example, once its estimated results are not accuracy enough, many useful speech components will be removed and irrelevant noise components will be reserved, which can heavily deteriorate the speech quality. More recently, a

great number of soft-decision T-F masks are proposed, which typically include ideal ratio mask (IRM) [14], ideal amplitude mask (IAM) [11], phase sensitive mask (PSM) [15] and complex ratio mask (CRM) [10]. Compared with IBM, soft masks can make a good balance between noise reduction and speech distortion. It has shown that one can obtain a better speech quality when using these soft-decision T-F masks [11].

In the previous fully connected (FC)-based noise reduction approaches, noisy features and clean labels are extracted in the frame format so that speech is enhanced frame by frame. Because of neglecting the structural characteristics of speech spectra and long contexts relations between frames, these approaches often result in spectral artifacts and speech distortion in high-frequency bands. To solve these problems, CNN-based and RNN-based models are recently investigated in this literature [8, 16, 17, 18, 19], which have shown to achieve better performance in both noise reduction and speech distortion. More recently, a type of advanced network named convolutional recurrent neural networks (CRNN) is proposed, which takes advantages of both CNNs and RNNs. It is shown that it can obtain a lower word error rate (WER) in speech recognition tasks [20] and later it is introduced into speech enhancement tasks [21, 22]. Compared with the single-type network, experiments have shown that the CRNN obtains better speech enhancement results.

Progressive learning (PL) has been introduced to the supervised speech enhancement algorithms [23, 24]. Essentially, it is a type of curriculum learning problem. Different from directly mapping from noisy features to clean targets, the whole process stage is divided into multiple easier and smaller stages, where the previous stage can boost the subsequent training processes. By doing so, the burden of the entire task can be distributed into each stage to effectively improve the performance of the whole network. In [23], the whole stage is divided into multiple stages so that within each stage, its target is to improve SNR to some degrees instead of directly recovering clean speech. Therefore, it is a type of multiple target learning (MTL). Compared with the FC-based network in [23], the network in [24] utilizes LSTM as the principal layer, which can

leverage long and short time dependencies to obtain more spectral information and also dense connection is helpful to further utilize previous stage outputs to guide the recovering of the next stage. For simplicity, architectures in the literature [23, 24] are referred as PL-DNN and PL-LSTM, respectively.

Although PL-DNN and PL-LSTM have shown its validity in improving speech quality, they still have some shortcomings for practical applications. First, compared with current advanced networks, pure DNNs and LSTMs are not so parameter-efficient. Too many parameters and too high computation complexity will limit the application in real-time scenarios. Second, in PL-DNN and PL-LSTM, only one specific layer (FC or LSTM) plays the major role in one sub-network, which is not so reasonable. This is because one layer is not adequate enough to map complicated nonlinear relations from one stage to the next. Third, the relations among different stages have not been fully explored yet. In a preliminary study, a weighted minimum mean square error (MMSE) loss criterion is adopted to train the network, where the first two weighting factors are fixed to 0.1 and 0.1, respectively, which is not convincing as weighting factors are relevant to the importance of sub-network for the whole network and a larger weighting factor means more emphasis is laid on the stage. Therefore, the influence of weighting factors should be fully explored.

To solve the above mentioned problems, we propose a novel progressive learning model to further improve the performance of speech enhancement especially under relatively low SNR conditions. The proposed model has several innovations when compared with the previous works. First, autoencoder-based CRNN is adopted as the sub-model within each stage instead of single FC layer or LSTM layer, which is more efficient for noise reduction formulation of one stage. To further exploit the parameters efficiently, we train the LSTM module in each stage recursively, i.e, the sub-models share the same LSTM parameters, which is suggested to reduce parameters while maintaining the performance. Second, we adopt causal convolution to formulate the architecture as a causal system, which has theoretical potential for real-time processing. Third, due to the fact that CNN layers can share weights by local sparse connections, it has much fewer

parameters than DNN and RNN layers. One can get that the proposed architecture has 77% and 93% reduction in parameter size, respectively, compared with PL-DNN and PL-LSTM. Fourth, we conduct extensive experiments to compare the performance of different training targets, including the magnitude of short-time Fourier transform (STFT) and multiple mask estimators. Finally, different weighting factor combinations are set up to explore the influence among several stages for the whole segregation process.

The remainder of this paper is organized as follows. In Section 2, the system flowchart is introduced briefly. Section 3 describes the training targets, and the CRNN-based model and its combination with progressive learning are also presented in this section. Section 4 presents the experimental settings. Section 5 gives the experimental results. Conclusion is presented in Section 6.

## 2. PROBLEM FORMULATION AND SYSTEM OVERVIEW

In time domain, a mixture signal is typically modeled as

$$x(t) = s(t) + n(t), \quad (1)$$

where  $x(t)$ ,  $s(t)$  and  $n(t)$  denote the noisy, the clean and the noise signals, respectively, in the time index  $t$ . From the perspective of frequency domain, the formula can be transformed into

$$X(k, l) = S(k, l) + N(k, l), \quad (2)$$

where  $X(k, l)$ ,  $S(k, l)$  and  $N(k, l)$  denote the noisy, the clean and the noise components, respectively, at the frequency bin index  $k$  and the time frame index  $l$ . Monaural speech enhancement aims to extract the clean speech component from the observed noisy mixture. For spectral mapping-based approaches, the output is the estimated clean speech spectral magnitude, which is denoted as  $|\widehat{S}|$ . For mask mapping-based approaches, mask  $\widehat{M}$  is estimated and can be used to estimate the clean speech spectral magnitude by multiplication operation.

The block diagram of progressive learning is shown in Figure 1. In the training stage, clean speech signals and interference noise signals are mixed together under various SNR conditions, where feature extraction and target

calculation are followed. One can see that we use  $X(k, l)$  to denote the feature and  $S_n(k, l)$  ( $n = 1, 2, 3$ ) to denote the target as an example. We adopt two types of targets herein, namely, the magnitude of spectrum and the mask. Multiple masks under different SNR-levels are sent to the DNN model as targets at different stages. In the testing stage, noisy features from test dataset are fed into the well-trained DNN model to estimate the desired targets in each T-F unit at different stages. After the clean speech spectral magnitude is estimated, overlap-add (OLA) technique is applied to reconstruct the speech signal in the time domain.

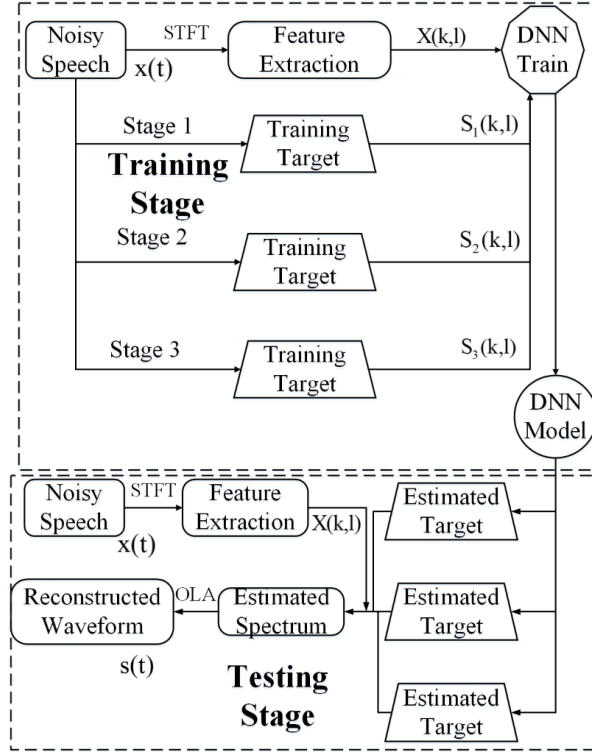


Figure 1: The block diagram of progressive learning.

### 3. ARCHITECTURE

#### 3.1. Features and Targets

In this study, the spectral magnitude of the noisy speech are extracted as the feature. PSM and IAM together with signal approximation (SA) are chosen as the mask targets for training, which are illustrated in Figure 2. Note that SA is essentially a type of mask analogous to IAM but its loss is defined as the distance between the spectral magnitude of the clean speech and that of the estimated clean speech. It has shown that SA-based approaches often lead to better performance in speech quality than mask approximation (MA)-based approaches [26]. In addition, to compare the performance between mask and spectral mapping methods, target magnitude spectrum (TMS) is also extracted as the training target. The value range of IAM and SA is  $(0, +\infty)$  if its value is not limited, we propose to truncate its value ranging from 0 to 1 to fit the range of the sigmoid function. Instead of truncating PSM into the range from 0 to 1 in [15], we truncate the value range of PSM into the range from -1 to 1 when considering that the mask can be both the positive value and the negative value due to that angle difference between noisy spectrum and clean spectrum can be a large value, so it is more reasonable to use double-side restriction method. For PSM, the tanh function is used as the activation function. Truncation is able to stabilize the training process by clipping. IAM, PSM and SA can be, respectively, given by

$$IAM(k, l) = \min \left\{ \max \left\{ \left| \frac{S(k, l)}{X(k, l)} \right|, 0 \right\}, 1 \right\}, \quad (3)$$

$$PSM(k, l) = \min \left\{ \max \left\{ \left| \frac{S(k, l)}{X(k, l)} \right| \cos(\theta_M(k, l)), -1 \right\}, 1 \right\}, \quad (4)$$

and

$$SA(k, l) = \left[ S(k, l) - X(k, l) \widehat{IAM}(k, l) \right]^2, \quad (5)$$

where  $\theta_M(k, l) = \angle S(k, l) - \angle X(k, l)$  denotes the phase difference between clean speech and noisy speech spectrum.  $\widehat{IAM}$  denotes the estimated IAM.

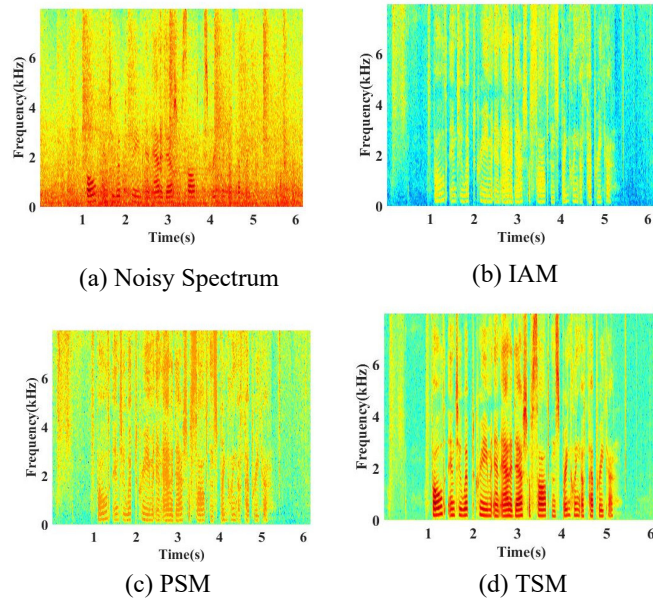


Figure 2: Illustration of IAM, PSM, and TMS. (a) the spectrum of noisy speech. (b) the IAM. (c) the PSM. (d) the target magnitude spectrum. SA is essentially a type of IAM except that the definition of its loss is different from IAM, and thus we only plot IAM for simplicity. The training targets (b), (c) and (d) are calculated under 0dB condition, where the noisy speech is mixed by a clean speech utterance taken from the TIMIT dataset and a factory noise taken from the NOISEX92 database.



### 3.2. Convolutional Recurrent Neural Network

Autoencoder-based CRNN is adopted as the sub-model. It resembles the architecture in [21] in which the principal part is convolutional encoder-decoder (CED) with LSTM playing as a bottleneck layer to capture time dependencies. In the encoding part, the size of feature map gradually decreases layer by layer, while in the decoding part the size gradually increases correspondingly, indicating the compression and the extension of features.

RNNs with gated mechanism and long short-term memory have been proposed to mitigate gradient vanishing and exploding issues when learning sequences with long time length. LSTM is a type of typical memory unit where different gates are set to control the percentage of saving, dropping temporal information, and receiving incoming information. Concrete calculation process is operated as follows:

$$\mathbf{i}_t = \sigma(\mathbf{W}_{ii}\mathbf{x}_t + \mathbf{b}_{ii} + \mathbf{W}_{hi}\mathbf{h}_{t-1} + \mathbf{b}_{hi}), \quad (6)$$

$$\mathbf{f}_t = \sigma(\mathbf{W}_{if}\mathbf{x}_t + \mathbf{b}_{if} + \mathbf{W}_{hf}\mathbf{h}_{t-1} + \mathbf{b}_{hf}), \quad (7)$$

$$\mathbf{g}_t = \tanh(\mathbf{W}_{ig}\mathbf{x}_t + \mathbf{b}_{ig} + \mathbf{W}_{hg}\mathbf{h}_{t-1} + \mathbf{b}_{hg}), \quad (8)$$

$$\mathbf{o}_t = \sigma(\mathbf{W}_{io}\mathbf{x}_t + \mathbf{b}_{io} + \mathbf{W}_{ho}\mathbf{h}_{t-1} + \mathbf{b}_{ho}), \quad (9)$$

$$\mathbf{c}_t = \mathbf{f}_t \odot \mathbf{c}_{t-1} + \mathbf{i}_t \odot \mathbf{g}_t, \quad (10)$$

$$\mathbf{h}_t = \mathbf{o}_t \odot \tanh \mathbf{c}_t. \quad (11)$$

where  $\mathbf{x}_t$ ,  $\mathbf{g}_t$ ,  $\mathbf{c}_t$  and  $\mathbf{h}_t$  refer to information input, block input, memory cell and hidden state at time  $t$ , respectively.  $\mathbf{W}$  and  $\mathbf{b}$  are weights and biases of the cell, respectively.  $\sigma(\bullet)$  and  $\tanh(\bullet)$ , respectively, denote the sigmoid and the tanh nonlinear functions.  $\odot$  represents element-wise product.

Causal convolution is first introduced in [27] for generating raw audio waveform and it achieves the state-of-the-art performance than all the previous models. During the calculation of the causal convolution, the predicted outputs emitted by the model is not relevant to the future information and only the

past temporal information is involved, and thus making it feasible for real-time processing in the speech enhancement task. An example of 2-D causal convolution is depicted in Figure 3. We use causal convolution in both the encoder and the decoder architectures as the deconvolution is essentially a type of convolution operation.

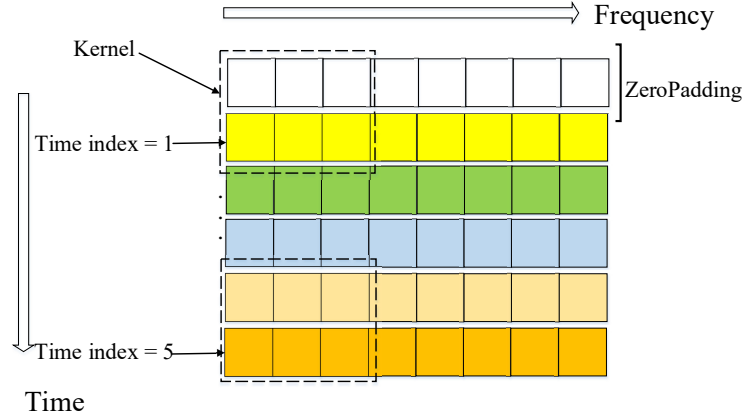


Figure 3: An example of causal 2-D convolution for speech enhancement task, which leads to a causal system. The size of kernel is set to (2,3) in the time and frequency axes, respectively. Zeropadding is applied before convolution to keep the size in time axes unchanged after convolution.

### 3.3. Proposed Architecture

The proposed progressive learning framework is shown in Figure 4, where the output target is the SA function as mentioned in (5) as an example. It is composed of three stages in the paper, where each sub-model is a type of convolutional recurrent autoencoder learning machine analogous to the network in [21] but with much fewer parameters. As stated in [24], PL leads to performance improvement but more learning targets may degrade the speech quality instead. Therefore, we fix the number of stages, i.e., 3, in this study. Within each stage,

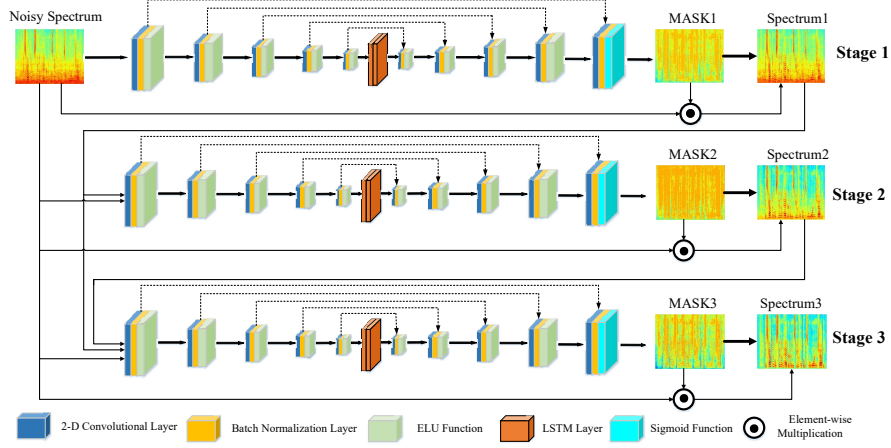


Figure 4: The architecture of proposed progressive learning framework. Only target SA is illustrated as an example for convenience. Different layers are identified with different color blocks as shown at the bottom of the figure. Dashed line indicates the skip operation.

there are three main components, including the convolutional encoder, the bottleneck LSTMs and the convolutional decoder. For the encoding part, it consists of five convolutional blocks, which creates a compressed and deep representation of the input features by halving the size of feature dimensions with striding operation in the frequency axes and doubling the number of channels layer. Each of the convolutional block is followed by batch normalization (BN) [28] and exponential linear unit (ELU) [29]. The decoder is a symmetric representation compared with the encoder, where the size of frequency feature gradually increases by applying deconvolution [30] and the number of channel decreases layer by layer. To compensate for the information loss caused by striding in the convolutional operation, high resolution features from the compressed path are combined with corresponding deconvolution layer by skip connections, which are also helpful to mitigate gradient vanishing problem.

Inspired by recent recursive concept in [31, 32] that part of the network is recursively utilized in the training, we propose to recursively utilize bottleneck

Table 1: Detailed parameter setup of proposed architecture. Our proposed model pasts three stages for progressive noise reduction, where each stage has nearly the same structure except that the input channel of each stage is different. We only show the parameter setup and tensor size of one stage for convenience.

layer name	input size	hyperparameters	output size
reshape_size.1	$T \times 161$	-	$1 \times T \times 161$
cascade.1	$1 \times T \times 161$	-	$n \times T \times 161$
conv2d.1	$n \times T \times 161$	$2 \times 3, (1, 2), 4$	$4 \times T \times 80$
conv2d.2	$4 \times T \times 80$	$2 \times 3, (1, 2), 8$	$8 \times T \times 39$
conv2d.3	$8 \times T \times 39$	$2 \times 3, (1, 2), 16$	$16 \times T \times 19$
conv2d.4	$16 \times T \times 19$	$2 \times 3, (1, 2), 32$	$32 \times T \times 9$
conv2d.5	$32 \times T \times 9$	$2 \times 3, (1, 2), 64$	$64 \times T \times 4$
reshape_size.2	$64 \times T \times 4$	-	$T \times 256$
lstm1	$T \times 256$	256	$T \times 256$
lstm2	$T \times 256$	256	$T \times 256$
reshape_size.3	$T \times 256$	-	$64 \times T \times 4$
deconv2d.1	$128 \times T \times 4$	$2 \times 3, (1, 2), 32$	$32 \times T \times 9$
deconv2d.2	$64 \times T \times 9$	$2 \times 3, (1, 2), 16$	$16 \times T \times 19$
deconv2d.3	$32 \times T \times 19$	$2 \times 3, (1, 2), 8$	$8 \times T \times 39$
deconv2d.4	$16 \times T \times 19$	$2 \times 3, (1, 2), 4$	$4 \times T \times 80$
deconv2d.5	$8 \times T \times 80$	$2 \times 3, (1, 2), 1$	$1 \times T \times 161$
reshape_size.4	$1 \times T \times 161$	-	$T \times 161$

LSTMs in different stages to further reduce the network parameters while maintaining the network performance. In other words, all the stages share the LSTM parameters during the training process and the testing process.

Different types of training targets are explored in this study, including the TMS, IAM, PSM and SA. When the network is for direct spectral mapping training, the output activation is softplus, which is a smooth representation of ReLU and also has shown its better training stabilization and performance in phoneme recognition tasks [33]. For truncated mask-based training, the sigmoid function or the tanh function is needed as the output activation function for each stage, depending on the value range.

For mask-based training targets, two approaches are proposed to recover spectral magnitudes using the estimated masks. We name the two approaches UNITER (non-iterative) method and ITER (iterative) method, respectively. For UNITER method, three mask definitions in each stage are calculated as:

$$IAM_n(k, l) = \min \left\{ \max \left\{ \left| \frac{S_n(k, l)}{X(k, l)} \right|, 0 \right\}, 1 \right\}, \quad (12)$$

$$PSM_n(k, l) = \min \left\{ \max \left\{ \left| \frac{S_n(k, l)}{X(k, l)} \right| \cos(\theta_{M_n}(k, l)), -1 \right\}, 1 \right\}, \quad (13)$$

$$SA_n(k, l) = \left[ S_n(k, l) - X(k, l) \widehat{IAM_n}(k, l) \right]^2, \quad (14)$$

where subscript  $n = 1, 2, 3$  denotes the stage index and  $S_n$  refers to the output spectrum in the stage  $n$ . Similarly, for ITER method, the mask definitions are as follows:

$$IAM_n(k, l) = \min \left\{ \max \left\{ \left| \frac{S_n(k, l)}{S_{n-1}(k, l)} \right|, 0 \right\}, 1 \right\}, \quad (15)$$

$$PSM_n(k, l) = \min \left\{ \max \left\{ \left| \frac{S_n(k, l)}{S_{n-1}(k, l)} \right| \cos(\theta_{M_n}(k, l)), -1 \right\}, 1 \right\}, \quad (16)$$

$$SA_n(k, l) = \left[ S_n(k, l) - S_{n-1}(k, l) \widehat{IAM_n}(k, l) \right]^2, \quad (17)$$

where  $S_0$  and  $S_3$  are two specific situations, representing original noisy spectrum (i.e.  $X$ ) and its clean version, respectively.

As the definitions above indicate, the former approach is non-iterative, where the denominator item remains unchanged during the calculation and the latter approach is iterative as both the numerator and the denominator items change at different stages.

A more detailed description of proposed progressive learning architecture can refer to Table 1. The network consists of three cascaded sub-models, where each sub-model is equipped with nearly the same architecture and parameter configurations. As a result, only the sub-model parameter setting is detailed provided in the table. The input and output size of 3-D tensor representation

are specified with  $(Channels \times Timestep \times FrequencyFeat)$  format and with  $(Timestep \times FrequencyFeat)$  for 2-D tensor representation. The hyperparameters are specified with  $KernelSize$ ,  $Stride$  and  $ChannelNumber$  format. It is noteworthy that cascade layer is applied for each sub-model, where the outputs in previous stages alongside with original noisy features are densely connected to increase the channel number in the current stage, which is analogous to the approach in [24]. For stage  $n$ , the number of input channel is set to  $n$  to satisfy the dense connection principle as shown in Table 1.

## 4. EXPERIMENTS

### 4.1. Datasets and Parameter Settings

Extensive experiments are conducted with the TIMIT corpus, which include 630 speakers of eight major dialects of American English with each reading tens utterances. Clean speech within dataset is split into the training, evaluation and testing datasets, respectively. Training dataset includes 4800 clean utterances under five different SNR levels (-10dB, -5dB, 0dB, 5dB and 10dB). 400 clean utterances are used for model evaluation and 200 independent utterances are randomly selected for model testing, both of which are mixed with noise under five mentioned SNR conditions. To our best knowledge, few speech enhancement models are trained under extremely low SNR condition especially to -10dB. Therefore, we can further investigate the robustness of the models. 115 types of noises are utilized for training, which incorporate 100 types of environmental noises in [34] and additional 15 types of noises from [6]. To explore the generalization capacity of the model, six unseen test noises are utilized, including babble, destroyerengine, factory1, factory2, m109 and white from NOISEX92 [35]. For each time, two types of randomly chosen noises are mixed with an clean utterance. In a word, a total of  $4800 (\text{speech}) \times 5 (\text{SNR}) \times 2 (\text{types}) = 48,000$ ,  $400 (\text{speech}) \times 5 (\text{SNR}) \times 2 (\text{types}) = 4,000$  contaminated utterances and their clean version pairs are built for training and evaluation, respectively. For both seen noise and unseen noise condition, totally  $200 (\text{speech}) \times 5 (\text{SNR})$

$\times 2$  (types) = 2,000 speech pairs are used for testing, where 2 refers to 2 types of noises chosen from 115 types of seen noise dataset and that of 15 types of unseen noise dataset.

The same feature extraction approach is adopted for both baselines and proposed model. The sampling rate is 16 kHz and 20-ms Hanning window function is applied with 10-ms overlap. A 320-point STFT is adopted, leading to a 161-D feature vector for each frame. Instead of extracting logarithm power spectrum (LPS), we use the magnitude of STFT for noisy speech as the feature, which is the same as [25, 21] for fair comparisons.

In the previous progressive-based works [23, 24], a weighted MMSE criterion is utilized to optimize all the parameters as different stages are involved in the training, i.e.,  $E = \sum_{n=1}^3 \alpha_n E_n$ , where  $E_n$  denotes the output loss in the stage  $n$  and  $\alpha_n$  is the weighted value of loss  $E_n$ , indicating the importance of the stage  $n$ . When back-propagation (BP) is operated, the loss calculated in each stage only impacts the network weights before the current layer. In [23, 24], the weighted values are fixed to 0.1 except the last stage. In this study, we set the weights to be 0.2 except the last stage. In the next Section, we will further explore the influence of different  $\alpha_n$  configurations on network performance.

#### 4.2. Comparison Methods

In our experiments, we compare our proposed model with another three baselines, i.e., progressive learning with feedforward DNN [23], LSTM-based progressive learning with dense connection [24] and autoencoder-based CRNN in real-time [25], which are termed as PL-DNN, PL-LSTM and CRNN, respectively. It is noteworthy that in [23], PL-DNN takes contextual 7 frames as the input and one frame as the output, where past and future information is both involved, which leads to the non-causal system. For fair comparison, we slightly transform all the baselines to be causal systems. For PL-DNN, previous 10 frames are combined with current frame to form a larger feature vector, i.e.,  $161 \times 11 = 1771$ . The structure of PL-DNN is  $\{2018 - 161 - 2048 - 161 - 2048 - 161\}$ , where the sigmoid function serves as the hidden activation function and the ReLU function

acts as the output activation function for each stage. Structure of PL-LSTM is  $\{1024 - 161 - 1024 - 161 - 1024 - 161\}$ , where 1024 refers to the number of LSTM units and 161 refers to the number of affine layers, which change both the feature dimension and value range. The output activation function on each stage is ReLU. Dense connection is utilized for PL-LSTM to increase its performance. Post-processing (PP) is applied to both PL-DNN and PL-LSTM to fully exploit the information from different stages. The value of  $\alpha$  follows the literature. CRNN from [25] is a type of powerful enhancement model, where the network is to map from noisy spectrum to clean spectrum. The model architecture is analogous to the proposed sub-model but with much more trainable parameters, i.e., the output channels of the encoder are 256 and the number of LSTM unit is 1024. All the progressive models are trained on three stages, each of which is to recover speech with 10dB, 10dB and infinite SNR value than the previous stage. Infinite SNR value here can be explained as the goal of the last stage is to recover the speech from one specified SNR condition to its clean version whose SNR can be approximately regarded as a very large value.

For proposed PL-CRNN approaches, multiple targets are used for comparison. For notation convenience, when UNITER approach is adopted, the training with *target* is called PL-CRNN+*target*+UNITER, and that of PL-CRNN+*target*+ITER when ITER approach is adopted. Note that when TMS is the target for PL-CRNN training, the system is called PL-CRNN+TMS as the two recovering approaches are only valid when the training target is the mask estimator.

Both baselines and proposed models are trained with Adam optimizer [36]. The learning rate is initialized at 0.001. We halve the learning rate only when consecutive 3 evaluation loss increment arises and the training process is early-stopped only if more than 10 increment on evaluation loss happens. Weighted MMSE is used as the training criterion. We train the model for 150 epochs to guarantee the model convergence. The minibatch is set to 16 at a utterance level. Within a minibatch, zero value is padded for all the utterances whose timestep length is less than the longest one. For PL-DNN, utterances from a



minibatch are reshaped into  $(Batch \times Timestep \times FrequencyFeat)$  format to meet the required input size.

## 5. RESULTS AND ANALYSIS

### 5.1. Evaluation Metrics

In this study, we evaluate the performance of different models in terms of speech quality and speech intelligibility with three objective metrics, containing perceptual evaluation of speech quality (PESQ) [37], short-time objective intelligibility (STOI) [38] and source-to-distortion ratio (SDR) [39].

### 5.2. Objective Results

Objective comparison results of different models are presented in Table 2 and Table 3 with seen noise and unseen noise conditions, respectively. The tables list the performance of the baselines and proposed models, where PL-DNN, PL-LSTM and CRNN are adopted as the baseline models, and PL-CRNN with different training targets and recovering approaches serve as the proposed models. From the tables, one can observe the following phenomena. (1) Both PL-DNN and PL-LSTM can effectively improve speech quality and intelligibility for both seen noise and unseen noise, which is consistent with the results in [23, 24], and PL-LSTM outperforms PL-DNN on different metrics in most cases. This can be explained from two aspects, where one is that LSTM layer is capable of utilizing long and short time dependencies across continuous frames while DNN layer can only obtain contextual information within a preset frame window, and the other is that, compared with PL-DNN, PL-LSTM takes advantage of the information from the previous estimate outputs by dense connections. (2) Compared with PL-DNN and PL-LSTM, our proposed model offers a obvious performance improvement for both seen noise and unseen noise, e.g., for seen noise, our proposed model with the best result achieve relative 0.55, 8.66% and 3.60 dB improvements over PL-DNN at SNR=-10 dB in terms of the PESQ, STOI and SDR, respectively. When it comes to unseen noise, despite the fact that all

the models suffer from performance degradation, our proposed model can still obtain promising results, i.e., 0.51, 7.5% and 2.15 dB performance improvement at most than PL-LSTM for -10dB SNR condition in terms of the PESQ, STOI and SDR, respectively. (3) Our proposed model does not have obvious superiority over CRNN baseline model and they are comparable in most cases. When the testing noise is within the training noise dataset, we find that CRNN outperforms our proposed model in terms of STOI, which shows that CRNN does better in improving the speech intelligibility, whereas our proposed model obtains better performance in terms of SDR for PL-CRNN+PSM+UNITER configuration. For unseen noise, CRNN obtains a close performance with PL-CRNN+TMS. However, one should note that, although PL-CRNN has the similar architecture structure with CRNN, it has with much fewer parameters, and thus can significantly reduce both the amount of parameters and the computational complexity. In other words, the results demonstrate that a model with a much larger number of parameters can be composed into several progressive stages, where each of which has a dramatically fewer parameters, but its performance can be maintained. (4) If comparing the two recovering approaches, i.e., UNITER approach and ITER approach, we find that PL-CRNN with the former approach tends to achieve better performance than PL-CRNN with the latter one. For both seen noise and unseen noise, when the training target is SA with UNITER approach, it outperforms other mask-based configurations generally, which also shows the advantages of signal approximation target. It is also worth noting that PL-CRNN+TMS produces the best results among all the PL-based architecture for unseen noise cases. This is because dense connection is adopted to the output mismatch, especially for target IAM and PSM. Dense connection will concatenate the previous outputs alongside with original noisy spectral magnitude into the input of current feature input.

Figures 5 to 8 present comprehensive evaluations for different models on different metrics. The results are calculated under five SNR conditions, with SNR = -10 dB, -5 dB, 0 dB, 5 dB, 10 dB. It can be seen that compared with the two factory noise cases, worse performance is obtained for babble noise, which

Table 2: Experimental results with seen noise in terms of the PESQ, the STOI and the SDR under different SNR conditions. **BOLD** indicates the best result in each column. Each result is the average value over 2000 testing experiments. For notation convenience, Alg.1: PL-CRNN+IAM+UNITER, Alg.2: PL-CRNN+PSM+UNITER, Alg.3: PL-CRNN+SA+UNITER, Alg.4: PL-CRNN+IAM+ITER, Alg.5: PL-CRNN+PSM+ITER, Alg.6: PL-CRNN+SA+ITER, Alg.7: PL-CRNN+TMS. It has the same notation system in the following tables.

Metrics	PESQ					STOI (in %)					SDR (in dB)				
SNR (dB)	-10	-5	0	5	10	-10	-5	0	5	10	-10	-5	0	5	10
Noisy	1.30	1.52	1.85	2.16	2.48	57.36	66.45	75.92	84.24	90.67	-9.80	-5.19	-2.68	4.67	9.66
PL-DNN	1.86	2.17	2.46	2.70	2.90	74.17	81.60	87.09	91.00	93.60	2.92	6.39	9.45	12.17	14.71
PL-LSTM	1.84	2.17	2.49	2.77	3.01	73.08	81.27	87.27	91.56	94.27	3.05	6.76	9.97	12.84	15.61
CRNN	2.39	<b>2.70</b>	<b>2.97</b>	3.23	3.44	82.77	<b>88.21</b>	<b>91.99</b>	<b>94.88</b>	<b>96.69</b>	6.07	8.77	11.53	14.33	17.21
Alg.1	2.27	2.57	2.85	3.14	3.40	80.85	86.25	90.56	93.92	96.11	4.61	7.52	10.56	13.66	16.92
Alg.2	2.23	2.60	2.92	<b>3.24</b>	<b>3.51</b>	76.90	83.94	89.23	93.28	95.81	<b>6.65</b>	<b>9.38</b>	<b>12.07</b>	<b>14.81</b>	<b>17.65</b>
Alg.3	<b>2.41</b>	2.69	2.95	3.21	3.43	<b>82.83</b>	87.77	91.52	94.44	96.44	6.06	8.83	11.67	14.53	17.63
Alg.4	1.87	2.19	2.49	2.80	3.08	73.80	80.56	86.21	91.07	94.39	1.75	5.25	8.65	12.01	15.47
Alg.5	2.11	2.45	2.74	3.05	3.32	75.05	81.83	87.17	91.62	94.60	4.66	7.48	10.20	13.14	16.08
Alg.6	2.26	2.57	2.85	3.13	3.37	78.08	85.56	90.17	93.73	95.99	5.96	8.74	11.47	14.35	17.39
Alg.7	2.25	2.57	2.81	3.06	3.26	81.10	86.86	90.77	93.84	95.92	5.57	8.42	11.19	13.96	16.80

Table 3: Experimental results with unseen noise in terms of the PESQ, STOI and SDR under different SNR conditions. **BOLD** indicates the best result in each column. Each result is the average value over 2000 testing experiments.

Metrics	PESQ					STOI (in %)					SDR (in dB)				
SNR (dB)	-10	-5	0	5	10	-10	-5	0	5	10	-10	-5	0	5	10
Noisy	1.08	1.33	1.66	2.02	2.38	45.35	55.98	67.60	78.85	87.77	-9.84	-5.17	-0.28	4.68	9.66
PL-DNN	1.06	1.42	1.84	2.24	2.60	45.41	59.21	72.53	82.95	89.81	-6.73	-2.05	5.19	9.61	13.43
PL-LSTM	1.29	1.71	2.11	2.47	2.79	52.51	66.01	77.51	85.94	91.43	-2.62	2.88	7.35	11.27	14.57
CRNN	1.36	1.80	2.25	<b>2.66</b>	<b>3.01</b>	54.14	68.68	<b>80.45</b>	<b>88.53</b>	<b>93.61</b>	-1.15	3.77	<b>8.04</b>	<b>11.98</b>	<b>15.71</b>
Alg.1	1.46	1.83	2.19	2.56	2.91	54.17	66.26	77.17	85.66	91.66	-2.50	2.64	6.99	11.04	14.99
Alg.2	1.26	1.70	2.17	2.54	2.91	47.69	61.42	74.33	84.08	90.90	-2.68	3.08	7.50	11.43	15.13
Alg.3	1.46	1.87	2.27	2.65	2.99	54.58	68.48	79.51	87.53	92.72	-1.64	3.50	7.77	11.80	15.65
Alg.4	1.22	1.65	2.09	2.48	2.83	50.78	63.85	75.36	84.14	90.50	-2.63	2.63	7.00	10.94	14.69
Alg.5	1.37	1.79	2.21	2.59	2.98	50.95	63.87	75.22	84.01	90.49	-1.20	3.82	7.82	11.35	14.86
Alg.6	1.47	1.86	2.26	2.60	2.93	53.78	67.55	78.60	86.72	92.20	-1.06	3.81	7.85	11.65	15.46
Alg.7	<b>1.59</b>	<b>1.95</b>	<b>2.29</b>	2.61	2.92	<b>60.01</b>	<b>70.75</b>	80.31	87.81	92.78	<b>-0.77</b>	<b>3.99</b>	8.01	11.87	15.54

can be explained that babble noise is a type of very unstationary noise and has the similar characteristic with speech signal, therefore it is more difficult to segregate the noise component from the noisy speech. Furthermore, we also find that all the approaches perform the worst for destroyerengine noise among four unseen noises. When comparing the performance among different models, one can observe that for factory and babble, PL-CRNN+TMS consistently outperforms three baselines whereas better results can be obtained with CRNN for the destroyerengine noise.

Figure 9 gives the spectrograms of an utterance contaminated by babble noise under 0 dB SNR condition and enhanced by six approaches, namely, PL-DNN, PL-LSTM, CRNN, PL-CRNN+TMS, PL-CRNN+SA+UNITER and PL-CRNN+SA+ITER. As seen from this figure, compared with PL-DNN and PL-LSTM, when convolutional recurrent neural network is taken, better restoration performance is offered, that is, the network can effectively recover the intermediate-frequency and high-frequency contents, which is typically lost in PL-DNN and PL-LSTM, as is shown in Fig. 9 (e), the dashed line box. When we compare CRNN and PL-CRNN, we find the latter network can better recover some spectral details, as the dashed line boxes show in Fig. 9 (f) and (g), which demonstrate the superiority of the proposed PL-CRNN.

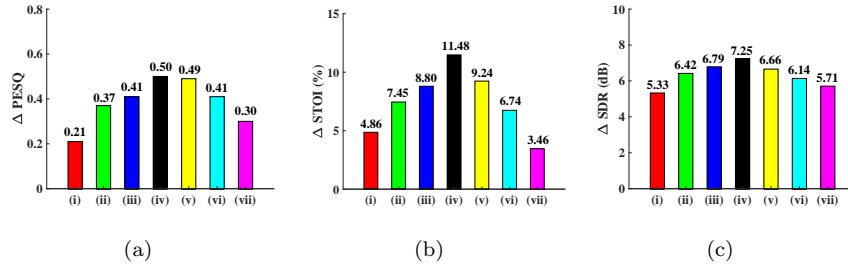


Figure 5: Average metric performance improvement for different architectures on unseen factory1 noise. The architectures are (i) PL-DNN, (ii) PL-LSTM, (iii) CRNN, (iv) PL-CRNN+TMS, (v) PL-CRNN+SA+UNITER, (vi) PL-CRNN+IAM+UNITER, (vii) PL-CRNN+PSM+UNITER. (a) The average performance on PESQ, (b) the average performance on STOI (in %), (c) the average performance on SDR (in dB).

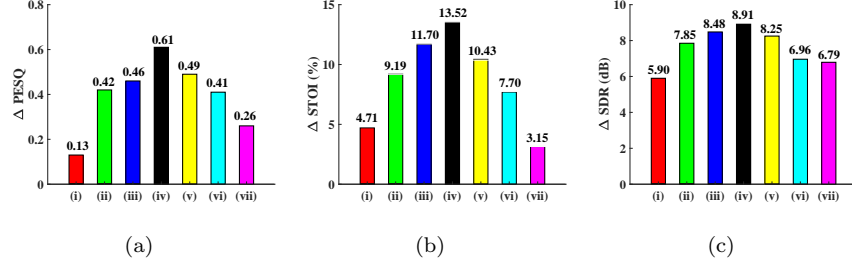


Figure 6: Average metric performance improvement for different architectures on unseen factory2 noise. The architectures are (i) PL-DNN, (ii) PL-LSTM, (iii) CRNN, (iv) PL-CRNN+TMS, (v) PL-CRNN+SA+UNITER, (vi) PL-CRNN+IAM+UNITER, (vii) PL-CRNN+PSM+UNITER. (a) The average performance on PESQ, (b) the average performance on STOI (in %), (c) the average performance on SDR (in dB).

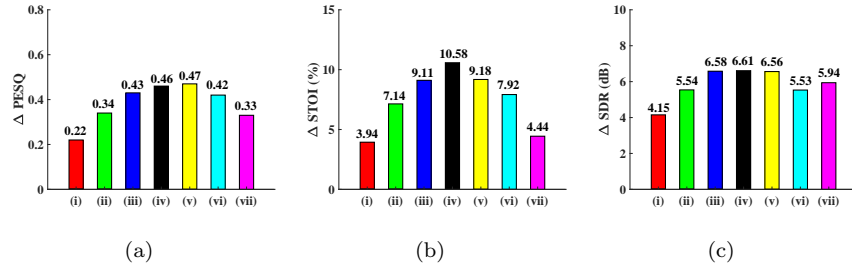


Figure 7: Average metric performance improvement for different architectures on unseen babble noise. The architectures are (i) PL-DNN, (ii) PL-LSTM, (iii) CRNN, (iv) PL-CRNN+TMS, (v) PL-CRNN+SA+UNITER, (vi) PL-CRNN+IAM+UNITER, (vii) PL-CRNN+PSM+UNITER. (a) The average performance on PESQ, (b) the average performance on STOI (in %), (c) the average performance on SDR (in dB).

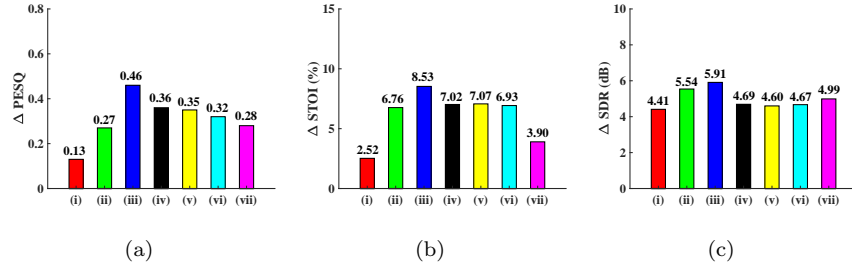


Figure 8: Average metric performance improvement for different architectures on unseen destroyer engine noise. The architectures are (i) PL-DNN, (ii) PL-LSTM, (iii) CRNN, (iv) PL-CRNN+TMS, (v) PL-CRNN+SA+UNITER, (vi) PL-CRNN+IAM+UNITER, (vii) PL-CRNN+PSM+UNITER. (a) The average performance on PESQ, (b) the average performance on STOI (in %), (c) the average performance on SDR (in dB).

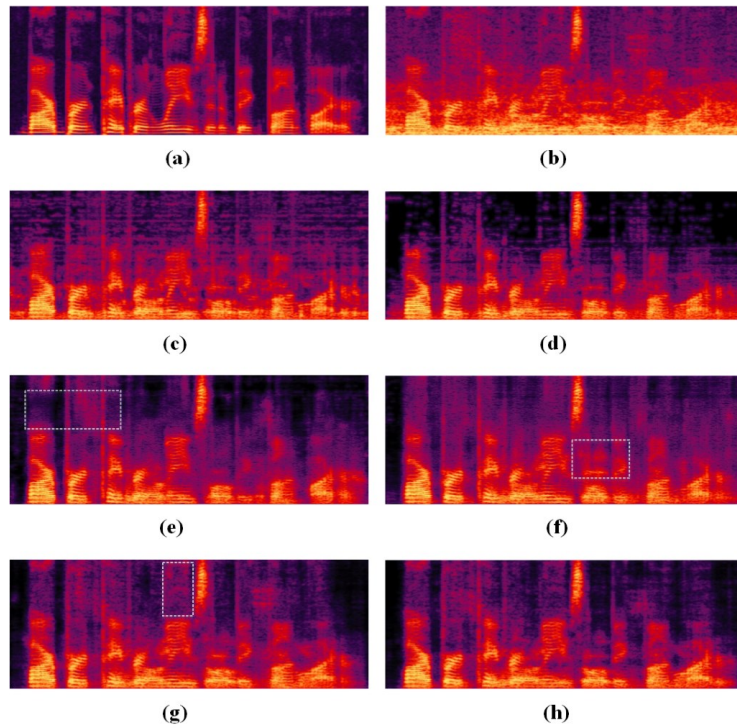


Figure 9: Spectrograms of an utterance contaminated by babble noise under 0dB SNR condition. (a) Clean speech, (b) Noisy speech, (c) PL-DNN, (d) PL-LSTM, (e) CRNN, (f) PL-CRNN+TMS, (g) PL-CRNN+SA+UNITER, (h) PL-CRNN+SA+ITER.

### 5.3. The Influence of $\alpha_n$

The influence of  $\alpha_n (n = 1, 2)$  to the network is explored. In the last part,  $\alpha_n$  is set to 0.2 except the last stage. The performance with different values of  $\alpha_n$  is shown in Figure 10 in terms of PESQ and STOI. From this figure, one can observe that the PESQ and the STOI scores gradually decrease with the increase of  $\alpha_n$ , indicating that the increase of  $\alpha_n$  instead has a negative impact on the network. This can be explained as the optimization goals of multiple stages are different and a relatively large  $\alpha_n$  value will have a negative effect on the previous stage parameter updating, leading to the optimization process deviation.  $\alpha_n = 0.1 (n = 1, 2)$  is the optimal value among different  $\alpha_n$  settings. It is noteworthy that  $\alpha_n = 0 (n = 1, 2)$  is a very special case where only one stage is involved.

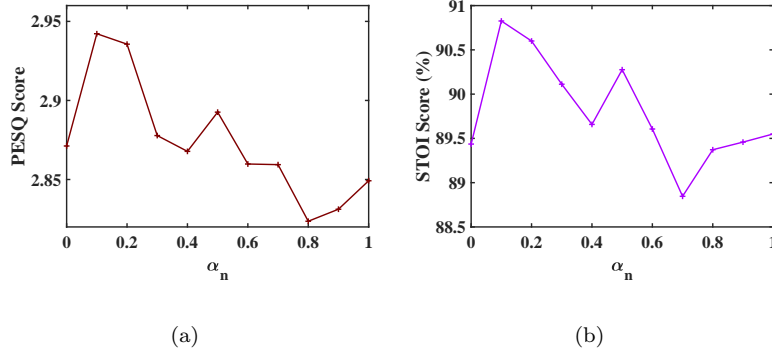


Figure 10: The performance of different  $\alpha_n (n = 1, 2)$  configurations. The target is SA with UNITER method and the testing value is evaluated on the seen noise.

### 5.4. Model Comparison

We compare different architectures in terms of the amount of parameters and the computational complexity, which are plotted in Figure 11. As the results show, the proposed PL-CRNN algorithm can significantly reduce the amount of parameters and flops compared with PL-DNN, PL-LSTM and CRNN.

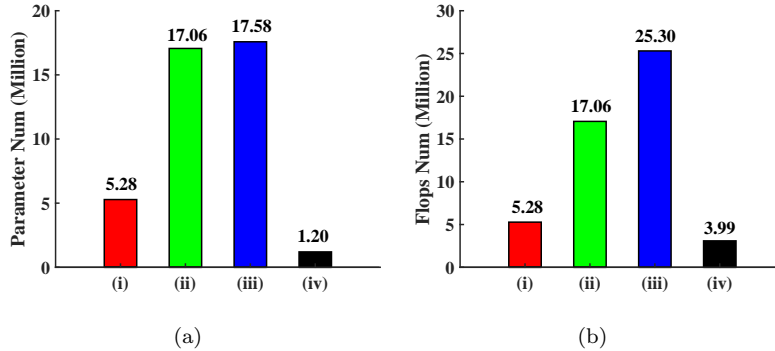


Figure 11: Comparisons on the amount of parameters and the computational complexity among different architecture. The values are presented in the million format. (i) PL-DNN, (ii) PL-LSTM, (iii) CRNN, (iv) PL-CRNN.

## 6. Conclusions

In this paper, we propose a progressive learning framework with CRNN, which takes advantages of both CNN and RNN to significantly reduce the amount of parameters and simultaneously improve speech quality and speech intelligibility compared with PL-DNN and PL-LSTM. To effectively recover the spectral magnitude of the clean speech, multiple training targets are adopted and two types of recovering approaches, namely, the UNITER method and the ITER method are proposed. Experimental results show that the proposed PL-CRNN algorithm obtains consistently better performance than the PL-DNN and PL-LSTM while has similar performance to CRNN in terms of PESQ, STOI and SDR.

## References

## References

- [1] P. C. Loizou, Speech enhancement: theory and practice, CRC press, 2013.
- [2] S. Boll, Suppression of acoustic noise in speech using spectral subtraction,



- IEEE Transactions on acoustics, speech, and signal processing. 27(2) (1979) 113–120.
- [3] J. Chen, J. Benesty, Y. Huang, S. Doclo, New insights into the noise reduction wiener filter, *IEEE Transactions on audio, speech, and language processing*. 14(4) (2006) 1218–1234.
  - [4] S. H. Jensen, P. C. Hansen, S. D. Hansen, J. A. Sorensen, Reduction of broad-band noise in speech by truncated qsvd, *IEEE Transactions on Speech and Audio Processing*. 3(6) (1995) 439–448.
  - [5] E. W. Healy, S. E. Yoho, Y. Wang, D. Wang, An algorithm to improve speech recognition in noise for hearing-impaired listeners, *The Journal of the Acoustical Society of America*. 134(4) (2013) 3029–3038.
  - [6] Y. Xu, J. Du, L.-R. Dai, C.-H. Lee, A regression approach to speech enhancement based on deep neural networks, *IEEE/ACM Transactions on Audio, Speech, and Language Processing*. 23(1) (2014) 7–19.
  - [7] Y. Xu, J. Du, L.-R. Dai, C.-H. Lee, Global variance equalization for improving deep neural network based speech enhancement, in: *2014 IEEE China Summit & International Conference on Signal and Information Processing (ChinaSIP)*, IEEE, 2014, pp. 71–75.
  - [8] S.-W. Fu, T.-y. Hu, Y. Tsao, X. Lu, Complex spectrogram enhancement by convolutional neural network with multi-metrics learning, in: *2017 IEEE 27th International Workshop on Machine Learning for Signal Processing (MLSP)*, IEEE, 2017, pp. 1–6.
  - [9] D. Wang, J. Chen, Supervised speech separation based on deep learning: An overview, *IEEE/ACM Transactions on Audio, Speech, and Language Processing*. 26(10) (2018) 1702–1726.
  - [10] D. S. Williamson, Y. Wang, D. Wang, Complex ratio masking for monaural speech separation, *IEEE/ACM Transactions on Audio, Speech and Language Processing (TASLP)*. 24(3) (2016) 483–492.

- [11] Y. Wang, A. Narayanan, D. Wang, On training targets for supervised speech separation, *IEEE/ACM transactions on audio, speech, and language processing*. 22(12) (2014) 1849–1858.
- [12] D. Wang, G. J. Brown, *Computational auditory scene analysis: Principles, algorithms, and applications*, Wiley-IEEE press, 2006.
- [13] D. Wang, On ideal binary mask as the computational goal of auditory scene analysis, in: *Speech separation by humans and machines*, Springer, 2005, pp. 181–197.
- [14] C. Hummersone, T. Stokes, T. Brookes, On the ideal ratio mask as the goal of computational auditory scene analysis, in: *Blind source separation*, Springer, 2014, pp. 349–368.
- [15] H. Erdogan, J. R. Hershey, S. Watanabe, J. Le Roux, Phase-sensitive and recognition-boosted speech separation using deep recurrent neural networks, in: *2015 IEEE International Conference on Acoustics, Speech and Signal Processing (ICASSP)*, IEEE, 2015, pp. 708–712.
- [16] S. R. Park, J. W. Lee, A fully convolutional neural network for speech enhancement, *Proc. Interspeech 2017* (2017) 1993–1997.
- [17] S.-W. Fu, Y. Tsao, X. Lu, Snr-aware convolutional neural network modeling for speech enhancement., in: *Interspeech*, 2016, pp. 3768–3772.
- [18] F. Weninger, H. Erdogan, S. Watanabe, E. Vincent, J. Le Roux, J. R. Hershey, B. Schuller, Speech enhancement with lstm recurrent neural networks and its application to noise-robust asr, in: *International Conference on Latent Variable Analysis and Signal Separation*, Springer, 2015, pp. 91–99.
- [19] J. Chen, D. Wang, Long short-term memory for speaker generalization in supervised speech separation, *The Journal of the Acoustical Society of America*. 141(6) (2017) 4705–4714.

- [20] R. Fakoor, X. He, I. Tashev, S. Zarar, Constrained convolutional-recurrent networks to improve speech quality with low impact on recognition accuracy, in: 2018 IEEE International Conference on Acoustics, Speech and Signal Processing (ICASSP), IEEE, 2018, pp. 3011–3015.
- [21] K. Tan, D. Wang, A convolutional recurrent neural network for real-time speech enhancement., in: Interspeech, 2018, pp. 3229–3233.
- [22] H. Zhao, S. Zarar, I. Tashev, C.-H. Lee, Convolutional-recurrent neural networks for speech enhancement, in: 2018 IEEE International Conference on Acoustics, Speech and Signal Processing (ICASSP), IEEE, 2018, pp. 2401–2405.
- [23] T. Gao, J. Du, L.-R. Dai, C.-H. Lee, Snr-based progressive learning of deep neural network for speech enhancement., in: INTERSPEECH, 2016, pp. 3713–3717.
- [24] T. Gao, J. Du, L.-R. Dai, C.-H. Lee, Densely connected progressive learning for lstm-based speech enhancement, in: 2018 IEEE International Conference on Acoustics, Speech and Signal Processing (ICASSP), IEEE, 2018, pp. 5054–5058.
- [25] K. Tan, J. Chen, D. Wang, Gated residual networks with dilated convolutions for monaural speech enhancement, *IEEE/ACM Transactions on Audio, Speech, and Language Processing*. 27(1) (2018) 189–198.
- [26] F. Weninger, J. R. Hershey, J. Le Roux, B. Schuller, Discriminatively trained recurrent neural networks for single-channel speech separation, in: 2014 IEEE Global Conference on Signal and Information Processing (GlobalSIP), IEEE, 2014, pp. 577–581.
- [27] A. van den Oord, S. Dieleman, H. Zen, K. Simonyan, O. Vinyals, A. Graves, N. Kalchbrenner, A. Senior, K. Kavukcuoglu, Wavenet: A generative model for raw audio, in: 9th ISCA Speech Synthesis Workshop, pp. 125–125.

- [28] S. Ioffe, C. Szegedy, Batch normalization: Accelerating deep network training by reducing internal covariate shift, in: International Conference on Machine Learning, 2015, pp. 448–456.
- [29] D.-A. Clevert, T. Unterthiner, S. Hochreiter, Fast and accurate deep network learning by exponential linear units (elus), arXiv preprint arXiv:1511.07289.
- [30] H. Noh, S. Hong, B. Han, Learning deconvolution network for semantic segmentation, in: Proceedings of the IEEE international conference on computer vision, 2015, pp. 1520–1528.
- [31] J. Kim, J. Kwon Lee, K. Mu Lee, Deeply-recursive convolutional network for image super-resolution, in: Proceedings of the IEEE conference on computer vision and pattern recognition, 2016, pp. 1637–1645.
- [32] D. Ren, W. Zuo, Q. Hu, P. Zhu, D. Meng, Progressive image deraining networks: a better and simpler baseline, in: Proceedings of the IEEE Conference on Computer Vision and Pattern Recognition, 2019, pp. 3937–3946.
- [33] H. Zheng, Z. Yang, W. Liu, J. Liang, Y. Li, Improving deep neural networks using softplus units, in: 2015 International Joint Conference on Neural Networks (IJCNN), IEEE, 2015, pp. 1–4.
- [34] G. Hu, D. Wang, A tandem algorithm for pitch estimation and voiced speech segregation, IEEE Transactions on Audio, Speech, and Language Processing. 18(8) (2010) 2067–2079.
- [35] A. Varga, H. J. Steeneken, Assessment for automatic speech recognition: Ii. noisex-92: A database and an experiment to study the effect of additive noise on speech recognition systems, Speech communication. 12(3) (1993) 247–251.
- [36] D. P. Kingma, J. Ba, Adam: A method for stochastic optimization, arXiv preprint arXiv:1412.6980.

- [37] A. W. Rix, J. G. Beerends, M. P. Hollier, A. P. Hekstra, Perceptual evaluation of speech quality (pesq)-a new method for speech quality assessment of telephone networks and codecs, in: 2001 IEEE International Conference on Acoustics, Speech, and Signal Processing. Proceedings (Cat. No. 01CH37221), Vol. 2, IEEE, 2001, pp. 749–752.
- [38] C. H. Taal, R. C. Hendriks, R. Heusdens, J. Jensen, An algorithm for intelligibility prediction of time–frequency weighted noisy speech, *IEEE Transactions on Audio, Speech, and Language Processing*. 19(7) (2011) 2125–2136.
- [39] E. Vincent, R. Gribonval, C. Févotte, Performance measurement in blind audio source separation, *IEEE transactions on audio, speech, and language processing*. 14(4) (2006) 1462–1469.